JOC The Journal of Organic Chemistry

Article

pubs.acs.org/joc

Synthesis and Isomeric Effects of Ladder-Type Alkylated Terbenzodithiophene Derivatives

Yung-Lung Chen, Jhih-Yang Hsu, Fang-Yu Lin, Yu-Ying Lai, Hsiao-Chieh Chou, and Yen-Ju Cheng*

Department of Applied Chemistry, National Chiao Tung University, 1001 University Road, Hsin-Chu, 30010 Taiwan

Supporting Information

ABSTRACT: A new class of heptacyclic ladder-type terbenzodithiophene (TBDT) structures merging three fused benzodithophenes was developed. Two TBDT conjugated isomers, named as *syn*-TBDT and *anti*-TBDT, where the two thienyl rings in the outmost BDT units are in the *syn*- and *anti*-fashion, are designed. Two decyl groups are introduced to their 6,13 and 7,14-positions to form four isomeric 6,13-*syn*-TBDT, 7,14-*syn*-TBDT, 6,13-*anti*-TBDT, and 7,14-*anti*-TBDT structures which are constructed by the DBU-induced 6-benzannulation involving propargyl-allenyl isomerization of the dieneyne moieties in the corresponding precursors followed by 6π-electrocyclization/aromatization, while isomeric TD-*syn*-TBDT and TD-*anti*-TBDT with four decyl groups substituted at 6,7,13,14-positions are synthesized via palladium-catalyzed dialkylacetylene insertion/C−H arylation of the corresponding iodobiaryl precursors. The intrinsic properties can be modulated by molecular manipulation of the main-chain and side-chain isomeric structures. *anti*-TBDT derivatives exhibit higher melting points, larger bandgaps, stronger intermolecular interactions, and higher mobility than the corresponding *syn*-TBDT analogues. These molecules can be further utilized as building blocks to make various TBDT-based materials for optoelectronic applications.

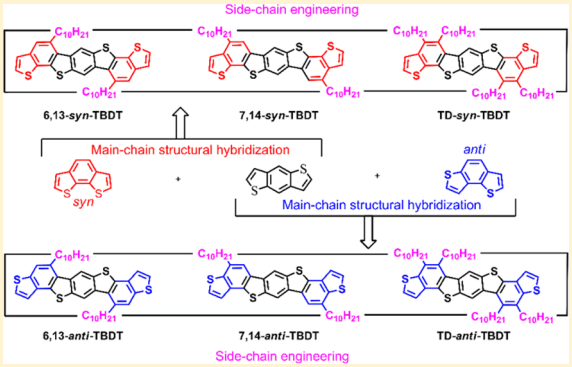

INTRODUCTION

The tricyclic benzodithiophene (BDT) family consists of isomeric structures such as benzo[1,2-*b*:4,5-*b*′]dithiophene, *anti*-form benzo[1,2-*b*:3,4-*b*′]dithiophene, and *syn*-form benzo[1,2-*b*:6,5-*b*′]dithiophene. Among them, benzo[1,2-*b*:4,5-*b*′]dithiophene unit is particularly one of the most successful building blocks to construct donor−acceptor copolymers for high-performance polymer solar cells due to its coplanar structure, high C_{2h} symmetry, and facile functionalization.[1] Covalently fastening adjacent aromatic and heteroaromatic subunits to form highly planar ladder-type conjugated structures leads to elongated effective conjugation, reduced optical bandgap, and enhanced intrinsic charge mobility.[2] It is of great interest to embed a BDT unit into a coplanar ladder-type structure that could possess superior molecular properties for the applications of organic transistors and photovoltaics. To this end, we recently designed and synthesized a dithienyl[1,2-*b*:4,5-*b*′]benzodithiophene-based heptacyclic ladder-type structure denoted as benzodi(cyclopentadithiophene) (BDCPDT) where the 3,7-positions of the central BDT subunit are covalently rigidified with the 3-positon of the two outmost thiophenes by two carbon bridges (Scheme 1).[3] The solar cells using a BDCPDT-based semiladder D−A copolymer exhibited higher power conversion efficiency compared to the corresponding nonfused polymer.[4] Due to the fact that the two carbon bridges in BDCPDT are a sp^3-hybridized atom, the two substituents at the carbon centers actually are out of the conjugation plane. Such steric hindrance will inevitably prevent the intermolecular $\pi-\pi$ interactions, which might deteriorate the charge transportation.[5]

With an aim to make a dithienylbenzodithiophene-based skeleton more planar, we come up with a new class of ladder-type structures where the central benzo[1,2-*b*:4,5-*b*′]dithiophenes unit is fastened with two outer thiophenes by two sp^2-sp^2 C=C bridges instead of the sp^3-carbon bridges. The resultant molecules are denoted as terbenzodithiophene (TBDT) since it actually merges three mutually fused benzodithophene units to form a heptacyclic arene (see Scheme 1). It has been documented that the isomeric geometry of a conjugated skeleton plays a significant role in governing the molecular stacking and structure ordering.[6] To investigate the isomeric conjugated effect, we design two TBDT isomers named as *syn*-TBDT and *anti*-TBDT where the two thiophene rings in the outmost BDT units are in the *syn*- and *anti*-fashion, respectively (see Scheme 1). Besides the conjugated main-chain engineering, the aliphatic side-chain engineering to ensure the solubility for solution processability also plays an equally important role.[7] The number of aliphatic chains and their attachment positions on a conjugated framework dramatically influence the solubility, crystallinity, and molecular assembly which eventually determine the thin-film morphology and

Received: January 15, 2016
Published: February 19, 2016

ACS Publications © 2016 American Chemical Society

DOI: 10.1021/acs.joc.6b00101
J. Org. Chem. 2016, 81, 2534−2542

Scheme 1. Molecular Structures of the Alkylated TBDT Derivatives

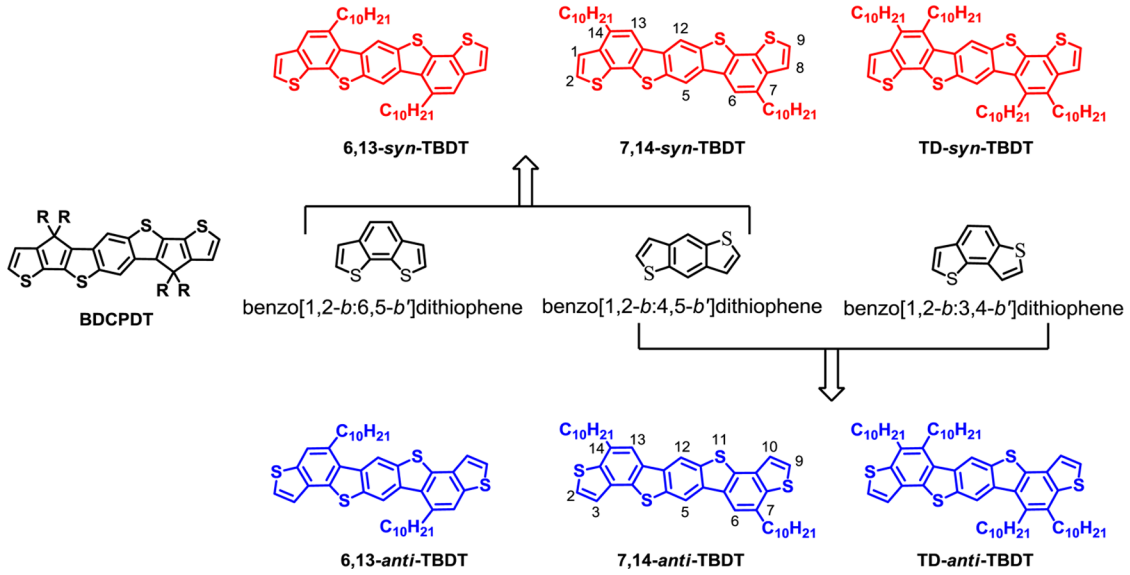

Scheme 2. Synthesis of 6,13-*syn*-TBDT and 6,13-*anti*-TBDT

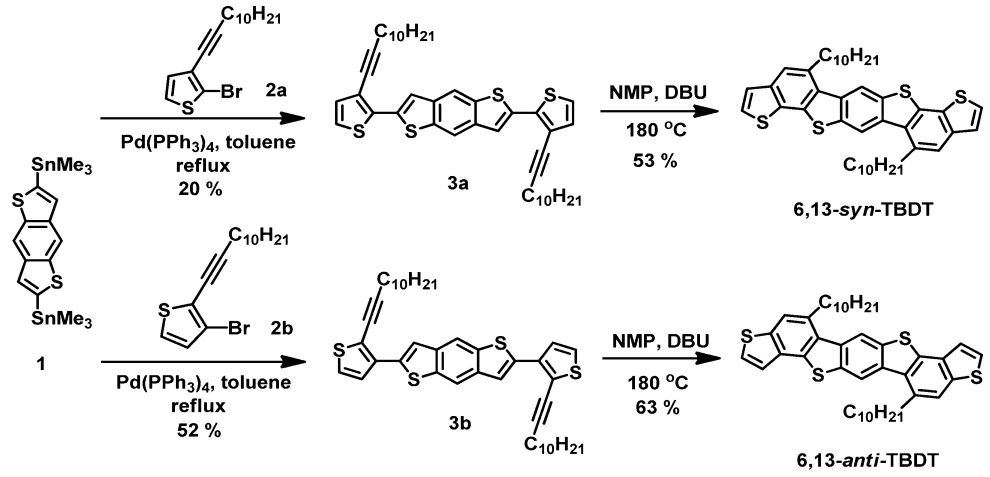

charge transportation.[7] However, introducing alkyl groups at the specific sp^2-carbons of a ladder-type π-system requires elegant synthetic strategy. In this research, we present a systematic synthesis to regiospecifically introduce two decyl groups at 6,13- or 7,14-positions of *syn*-TBDT and *anti*-TBDT frameworks, forming four isomeric didecyl TBDT molecules symbolized as 6,13-*syn*-TBDT, 7,14-*syn*-TBDT, 6,13-*anti*-TBDT, and 7,14-*anti*-TBDT (Scheme 1). Furthermore, a facile methodology is developed to successfully incorporate four decyl groups at 6, 7, 13, and 14 positions to form 6,7,13,14-*syn*-TBDT and 6,7,13,14-*anti*-TBDT denoted as TD-*syn*-TBDT and TD-*anti*-TBDT (Scheme 1, TD stands for tetradecyl groups). The molecular properties and isomeric effects of the six compounds have been systematically characterized and analyzed.

RESULTS AND DISCUSSION

The synthesis of 6,13-*syn*-TBDT and 6,13-*anti*-TBDT is shown in Scheme 2. Stille coupling of 2,6-bis(trimethylstannyl) BDT (**1**) with 2-bromo-3-(dodec-1-yn-1-yl)thiophene (**2a**) or 3-bromo-2-(dodec-1-yn-1-yl)thiophene (**2b**) resulted in the formation of **3a** and **3b**, respectively. **3a** and **3b** underwent double intramolecular annulation in the presence of 1,8-diazabicyclo[5.4.0]undec-7-ene (DBU) to afford 6,13-*anti*-TBDT and 6,13-*anti*-TBDT. The proposed mechanism involves the DBU-induced propargyl-allenyl isomerization followed by 6π-electrocyclization/aromatization.[8] The synthesis of 7,14-*syn*-TBDT and 7,14-*anti*-TBDT is shown in Scheme 3. Palladium-catalyzed Sonogashira coupling reactions of 1,4-diethynyl-2,5-dithiomethylbenzene (**4**) with 2-iodothiophene (**5a**) or 3-iodothiophene (**5b**) yielded compound **6a** and **6b**, respectively. Treatment of **6a** and **6b** with iodine generated the central iodinated BDT moieties in the compound **7a** and **7b**, which further carried out Sonogashira coupling reactions with 1-dodecyne to furnish compound **8a** and **8b**, respectively. In a similar manner, DBU-assisted cyclization of compound **8** yielded the 7,14-*syn*-TBDT and 7,14-*anti*-TBDT with the decyl groups regiospecifically attached at 7 and 14 positions.

The synthesis of tetraalkylated TBDT molecules is depicted in Scheme 4. A known protocol to make similar compounds adopts the four-fold Suzuki–Miyaura coupling reaction of 1,2-(diboronic ester)-1,2-dialkylethylene with a tetrabrominated arene.[9] However, preparation of these precursors requires more tedious synthesis. Palladium-catalyzed benzannulation between

DOI: 10.1021/acs.joc.6b00101
J. Org. Chem. 2016, 81, 2534–2542

Scheme 3. Synthesis of 7,14-*syn*-TBDT and 7,14-*anti*-TBDT

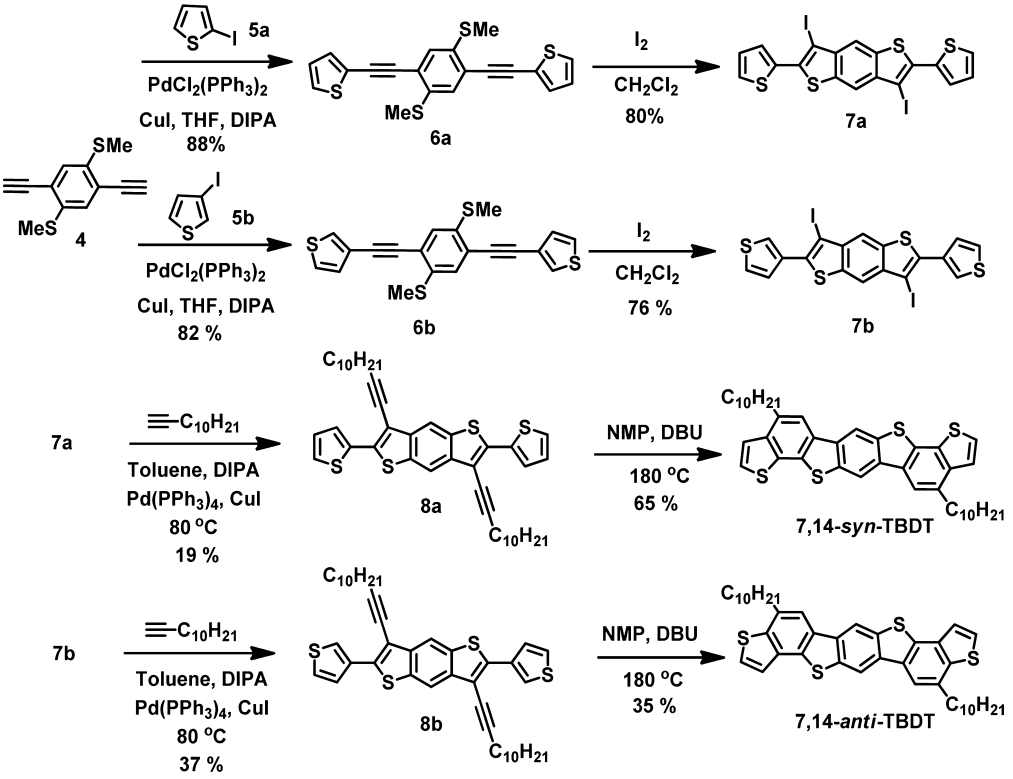

Scheme 4. Synthesis of TD-*syn*-TBDT and TD-*anti*-TBDT

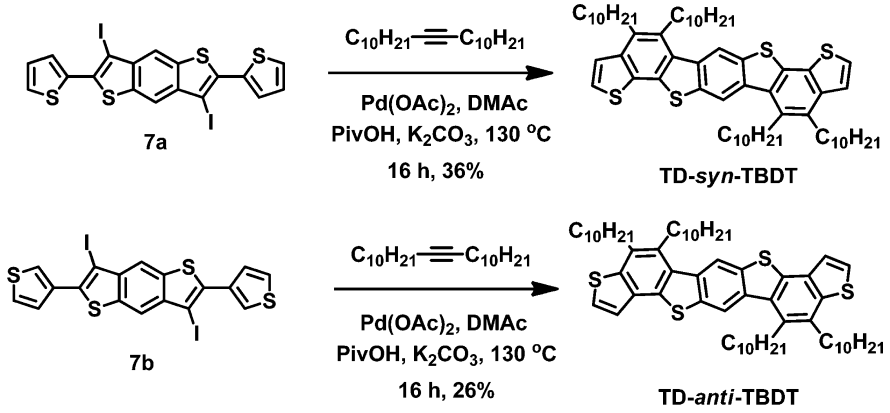

an iodobiaryl and a diphenylacetylene has been described.[10] Nevertheless, using a 1,2-dialkylacetylene substrate for the reaction to construct *ortho*-dialkylbenzene moiety is more challenging and thus remains unreported. Herein, we present an easy and expedited way to construct a tetraalkylated TBDT in one step by employing a palladium-catalyzed transformation. In the presence of $Pd(OAc)_2$ and pivalic acid in dimethylacetamide (DMAc), reaction of 1,2-decylacetylene with compound **7a** having the 2-thienyl moieties successfully resulted in the formation of benzodithiophene units in TD-*syn*-TBDT with introducing four decyl groups at 6, 7, 13, and 14 positions. The structure of TD-*syn*-TBDT is unambiguously confirmed by its single-crystal X-ray crystallography shown in Figure 1. Under identical catalytic conditions, **7b** with 3-thienyl moieties also furnished the isomeric TD-*anti*-TBDT product. The reaction mechanism involves oxidative addition of diiodoarenes **7** to palladium catalyst followed by *syn*-insertion of alkyne to form a resulting vinylic palladium intermediate which undergoes activated C−H arylation with the neighboring 2-thienyl or 3-thienyl rings.[11] It is envisaged that this transformation can have a broad scope for both iodobiaryl and dialkylacetylene substrates to make various alkylated polycyclic aromatic hydrocarbons. The molecular properties of the six compounds are summarized in Table 1.

Differential scanning calorimetry (DSC) of the six molecules is shown in Figure 2. All the molecules showed distinct melting points (T_m) upon heating and crystallization points upon cooling, indicating their highly crystalline nature. Melting points of the materials are highly associated with their main-chain and side-chain structural variations. Systematic trends are observed as follows: (1) *anti*-TBDT derivatives have higher T_m than the corresponding *syn*-TBDT analogues (191 °C for 6,13-*anti*-TBDT > 127 °C for 6,13-*syn*-TBDT; 234 °C for 7,14-*anti*-TBDT > 178 °C for 7,14-*syn*-TBDT; 150 °C for TD-*anti*-

DOI: 10.1021/acs.joc.6b00101
J. Org. Chem. 2016, 81, 2534−2542

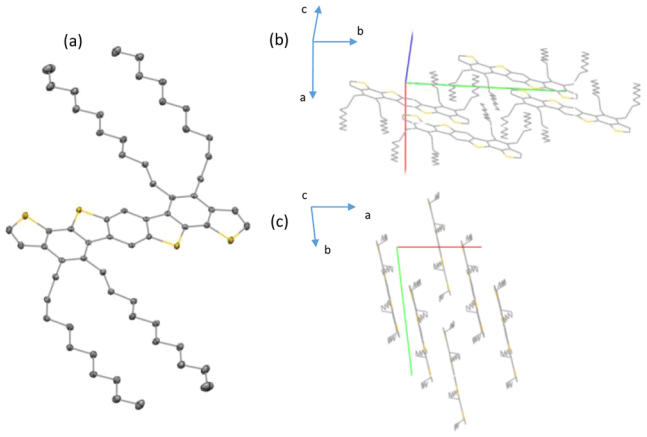

Figure 1. (a) ORTEP drawing of TD-*syn*-TBDT. Thermal ellipsoids are set at 50% probability; (b) intermolecular packing; and (c) packing along the *c* axis.

Table 1. Molecular Properties of the Six TBDT Compounds

molecules	T_m (°C)[a]	T_c (°C)[b]	T_d (°C)[c]	λ_{max} (nm)	λ_{onset} (nm)	E_g^{opt} (eV)	HOMO (eV)
6,13-*syn*-TBDT	127	69	422	282, 347, 378	389	3.19	−5.60
7,14-*syn*-TBDT	178	152	398	282, 349, 378	392	3.17	−5.55
TD-*syn*-TBDT	102	74	454	282, 351, 385	396	3.13	−5.54
6,13-*anti*-TBDT	191	140	406	282, 334, 370	380	3.27	−5.60
7,14-*anti*-TBDT	234	224	433	282, 337, 370	382	3.25	−5.52
TD-*anti*-TBDT	150	96	426	283, 336, 375	388	3.19	−5.50

[a] T_m: melting point. [b] T_d: crystallization point. [c] T_d: decomposition temperature.

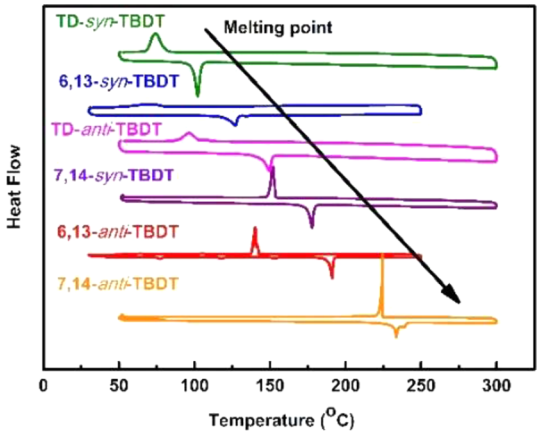

Figure 2. DSC of the six molecules at a ramping rate of 10 °C/min.

TBDT > 102 °C for TD-*syn*-TBDT); (2) 7,14-TBDT derivatives with outer alkylation have higher T_m than the 6,13-TBDT counterparts with inner alkylation (234 °C for 7,14-*anti*-TBDT > 191 °C for 6,13-*anti*-TBDT; 178 °C for 7,14-*syn*-TBDT > 127 °C for 6,13-*syn*-TBDT); and (3) tetraalkylated TD-*syn*-TBDT and TD-*anti*-TBDT exhibit the lower T_m compared to their dialkylated analogues. According to the aforementioned comparison, it is intriguing to observe that the T_m of TD-*syn*-TBDT, 6,13-*syn*-TBDT, TD-*anti*-TBDT, 7,14-*syn*-TBDT, 6,13-*anti*-TBDT, and 7,14-*anti*-TBDT are steadily increased with a rough linear relationship (Figure 2).

The profiles of the absorption spectra are mainly governed by the main-chain isomeric structure (Figure 3). The *syn*-

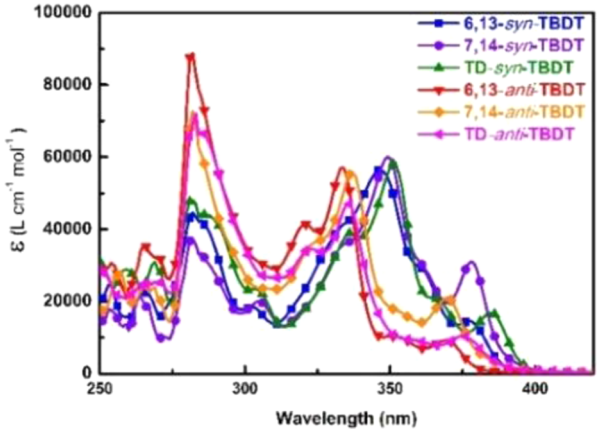

Figure 3. Absorption spectra of six TBDT-based molecules in dichloromethane with the concentration of ca. 10^{-5} M.

TBDT derivatives showed more red-shifted absorption bands than the *anti*-TBDT molecules, suggesting the *syn*-form has more effective conjugated length than the *anti*-form. It is noteworthy that the DT-TBDTs with four electron-donating alkyl groups exhibited the smallest optical bandgaps than the corresponding dialkylated molecules.

Cyclic voltammetry (CV) was employed to examine the electrochemical properties and determine the highest occupied molecular orbital (HOMO) (Figure 4). The HOMO energy

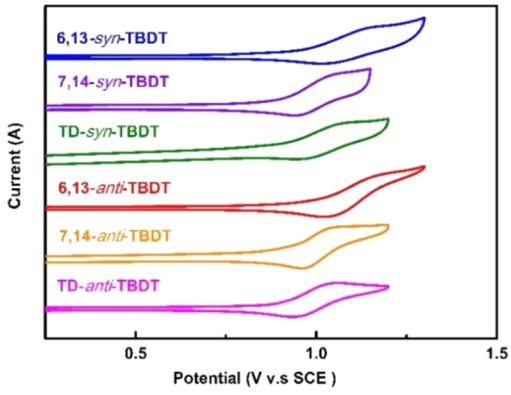

Figure 4. Cyclic voltammograms of the six TBDT-based molecules at a scan rate of 50 mV/s.

levels of the materials were determined to be from −5.50 to −5.60 eV. The tetraalkylated TBDTs have slightly higher HOMO levels than the dialkylated TBDTs due to the electron-donating decyl groups, while the 7,14-TBDTs also have slightly higher HOMO levels than the 6,13-TBDT counterparts.

DFT calculations were carried out at the TD-B3LYP/6-311G (d,p), PCM = toluene//B3LYP/6-311G (d,p) level of theory to elucidate the electronic structure of TBDT-series compounds. The decyl groups are replaced with the ethyl groups due to the fact that the length of aliphatic side chain has negligible impact on the electronic structure for rigid conjugated molecules. Computed HOMO/LUMO energy, excitation energy, oscillator strength, and configuration of the excited states are

DOI: 10.1021/acs.joc.6b00101
J. Org. Chem. 2016, 81, 2534−2542

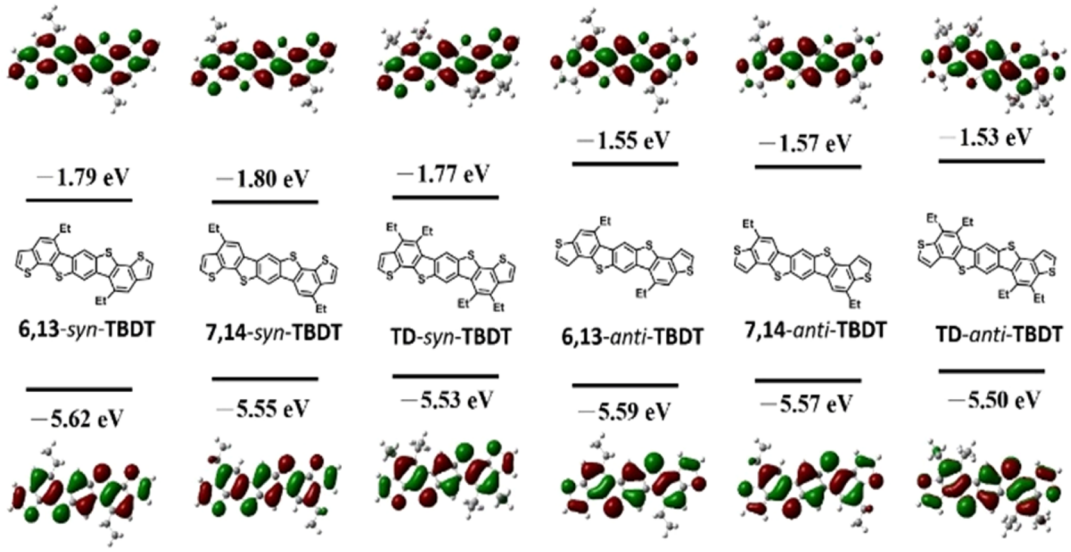

Figure 5. Plots of calculated molecular frontier orbitals for the TBDT-series compounds.

summarized in Table S1. Calculated molecular frontier orbitals contours and HOMO/LUMO levels are depicted in Figure 5. The calculated HOMO energy levels are in good correlation with the experimental values. The involvement of alkyl groups in the HOMO in the tetraalkylated TBDTs is also supported by the HOMO plots depicted in Figure 5. The theoretical LUMO values of *syn*-TBDTs are all lower than those of *anti*-TBDTs. The LUMO contours in Figure 5 reveal that the $C_2{=}C_3$ ($C_9{=}C_{10}$) double bonds of the outmost thiophenes in *anti*-TBDTs have low electron density, which may result in the more restricted LUMO electron distribution and thus higher LUMO energy for *anti*-TBDTs.

Single-crystal structures and intermolecular packings of 6,13-*anti*-TBDT and 6,13-*syn*-TBDT determined by X-ray crystallography are described in Figures 6 and 7, respectively.

The $\pi{-}\pi$ stacking distance of 6,13-*syn*-TBDT and 6,13-*anti*-TBDT is 3.40 and 3.28 Å, respectively, indicating that 6,13-*anti*-TBDT has closer packing. As deduced from crystal packing, each molecule is surrounded by six equivalents (Table S2). On the basis of symmetry operation, the intermolecular interactions

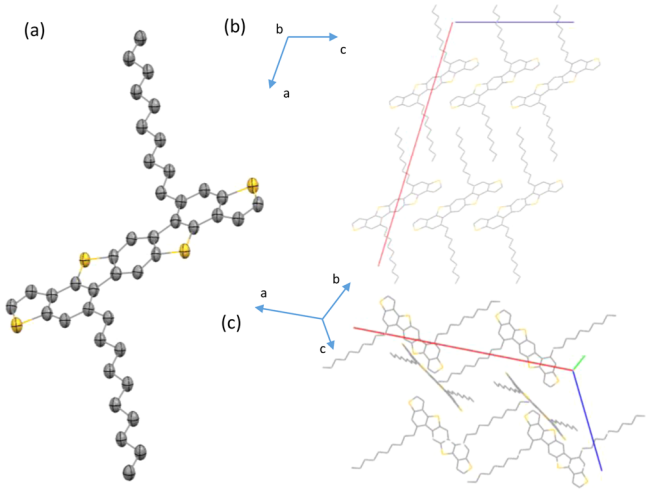

Figure 6. (a) ORTEP drawing of 6,13-*anti*-TBDT. Thermal ellipsoids are set at 50% probability. (b) and (c) Intermolecular packing.

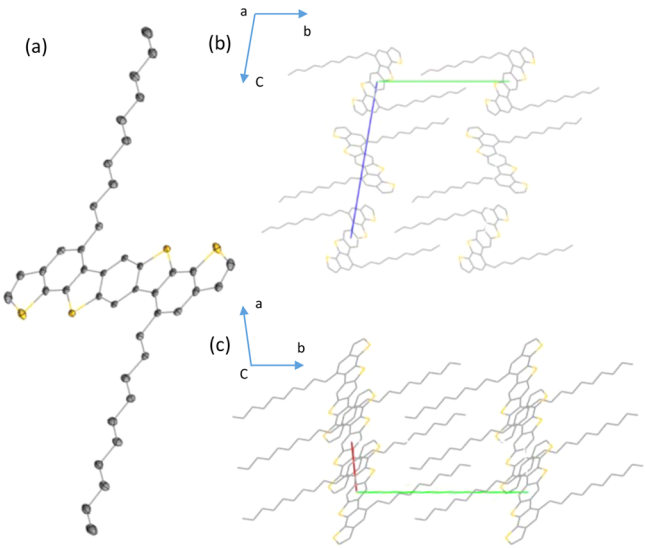

Figure 7. (a) ORTEP drawing of 6,13-*syn*-TBDT. Thermal ellipsoids are set at 50% probability. (b) and (c) Intermolecular packing.

in the 6,13-*syn*-TBDT and 6,13-*anti*-TBDT crystals can be classified into t_a, t_p, and t_q, where t_a is the intermolecular interactions along the molecular stacking direction, while t_p and t_q are the peripheral interactions (Figure 8 and Table S2). Extended transition-state natural orbitals for chemical valence (ETS-NOCV) analysis at the BP86-BJDAMP/TZP level of theory was then carried out to quantify the energy of t_a, t_p, and

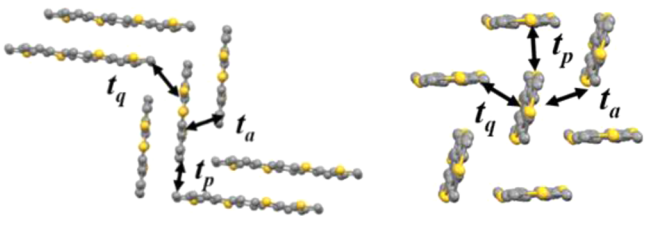

Figure 8. BP86-BJDAMP/TZP ETS-NOCV analysis of the intermolecular interaction existing in the 6,13-*syn*-TBDT and 6,13-*anti*-TBDT crystals. The alkyl chains are omitted for clarity.

DOI: 10.1021/acs.joc.6b00101
J. Org. Chem. 2016, 81, 2534−2542

t_q. The results are listed in Table S2. The interaction energy (ΔE_{int}) is treated as an entity to estimate the intermolecular interaction energy. ΔE_{int} can be decomposed into electrostatic interaction (ΔE_{elst}), Pauli repulsion (ΔE_{Pauli}), orbital interaction (ΔE_{oi}), and dispersion (ΔE_{dis}). It is evident that the principal stabilization in 6,13-*anti*-TBDT and 6,13-*syn*-TBDT comes from ΔE_{dis}, which is medium- to long-range intermolecular interactions. Moreover, the ΔE_{int} values of 6,13-*anti*-TBDT in t_a, t_p, and t_q directions are all higher than those of 6,13-*syn*-TBDT, strongly suggesting that 6,13-*anti*-TBDT possesses stronger intermolecular interactions in the solid state than 6,13-*syn*-TBDT. One of the possible reasons accounting for this result is associated with the intersection angle between the molecular plane and the aliphatic side chains (7° for 6,13-*anti*-TBDT and 31° for 6,13-*syn*-TBDT, Figures 6 and 7). Small intersection angle in 6,13-*anti*-TBDT reduces the steric hindrance between the conjugated moieties, leading to closer intermolecular packing and greater intermolecular interactions. The theoretical results can rationalize that 6,13-*anti*-TBDT has a higher melting point than 6,13-*syn*-TBDT.

TD-*anti*-TBDT and TD-*syn*-TBDT with higher solubility were chosen for the fabrication of solution-processed bottom-gate/top-contact field-effect transistors (OFETs) to preliminarily evaluate their charge mobility. The OFETs using SiO_2 as gate dielectric were treated with octadecyltrichlorosilane (ODTS) to form a self-assembly monolayer. The hole mobility was deduced from the transfer characteristics of the devices in the saturation regime as shown in Figure 9. TD-*anti*-TBDT exhibited a higher hole mobility of 8.16×10^{-2} cm^2 V^{-1} s^{-1} ($I_{on}/I_{off} = 1.55 \times 10^5$, $V_{th} = -49.7$ V) than TD-*syn*-TBDT with a mobility of 4.63×10^{-3} cm^2 V^{-1} s^{-1} ($I_{on}/I_{off} = 1.83 \times 10^5$, $V_{th} = -44.4$ V). This result is in good agreement with the stronger intermolecular interactions in the *anti*-form isomer than in the *syn*-form counterpart.

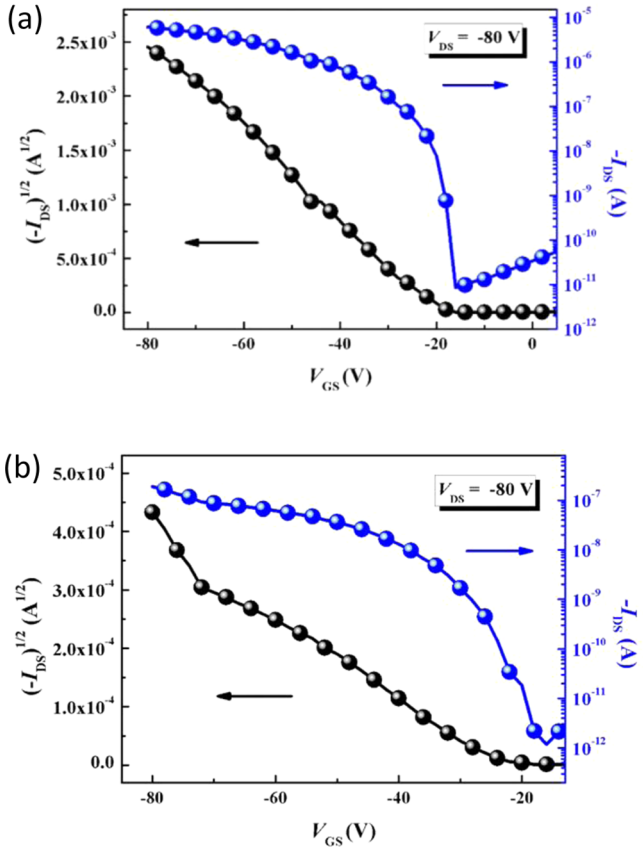

Figure 9. Transfer plots of the OFET devices based on (a) TD-*anti*-TBDT and (b) TD-*syn*-TBDT.

CONCLUSIONS

In summary, a new class of heptacyclic ladder-type terbenzodithiophene structures merging three fused benzodithophenes was designed and synthesized. Four dialkylated 6,13-*syn*-TBDT, 7,14-*syn*-TBDT, 6,13-*anti*-TBDT, and 7,14-*anti*-TBDT molecules were prepared via the DBU-induced 6π-cyclization of the corresponding dieneyne-based precursors, while two tetraalkylated TD-*syn*-TBDT and TD-*anti*-TBDT were synthesized via palladium-catalyzed alkyne insertion/C−H arylation of the iodobiaryl precursors. It is envisaged that these synthetic methodologies can be adopted to prepare other ladder-type conjugated backbones with precise introduction of aliphatic side chains for solution processabiity. The molecular properties of the molecules can be modulated by molecular manipulation of the main-chain and side-chain isomeric structures. The *anti*-TBDTs show the higher melting points, larger bandgaps, and stronger intermolecular interactions than the corresponding *syn*-TBDTs. Specifically, TD-*anti*-TBDT exhibited a higher OFET mobility than TD-*syn*-TBDT by 1 order of magnitude. These molecules can be further utilized as building blocks to make versatile TBDT-based materials for solution-processable organic transistors and solar cells.

EXPERIMENTAL SECTION

General Measurements and Characterization. Unless otherwise stated, all reactions were carried out on a vacuum line under N_2 atmosphere. ^1H and ^{13}C NMR spectra were measured using a 400 MHz instrument spectrometer and obtained in deuterated chloroform ($CDCl_3$) with TMS as internal reference unless otherwise stated, and chemical shifts (δ) are reported in parts per million. DSC was measured under nitrogen atmosphere at a heating rate of 10 °C/min. Thermogravimetric analysis (TGA) was recorded under a nitrogen atmosphere at a heating rate of 10 °C/min. Cyclic voltammetry was conducted on an electrochemical analyzer. A carbon glass was used as the working electrode, Pt wire was used as the counter electrode, and Ag/Ag^+ electrode (0.01 M $AgNO_3$, 0.1 M TBAP in dichloromethane) was used as the reference electrode in a solution of dichloromethane with 0.1 M $TBAPF_6$ (tetrabutylammonium hexafluorophosphate) at a ramping rate of 10 mV/s. CV curves were calibrated using ferrocene as the standard, $E(\text{ferrocene})_{onset} = 0.02$ V. The HOMO energy levels were obtained from the equation: HOMO = $-(E_{ox\ onset} - E(\text{ferrocene})_{onset} + 4.8)$ eV. The optical band gaps (E_g^{opt}) were calculated from the absorption onset of the solution state by using the equation of $E_g^{opt} = 1240/\lambda_{onset}$.

Synthesis of ***3a****.* To a 100 mL two-neck bottom flask, compound **1** (1 g, 1.9 mmol), 2-bromo-3-(dodec-1-yn-1-yl)thiophene **2a** (1.52 g, 4.65 mmol), $Pd(PPh_3)_4$ (0.11 g, 0.096 mmol), and degassed toluene (40 mL) were introduced. The mixture was reacted at 130 °C under nitrogen for 48 h. After removal of solvent by a rotary evaporator, the residue was purified by column chromatography on silica gel (hexane/ethyl acetate, v/v, 50/1). The compound was dissolved in hexane at 60 °C. The solution was cooled down to room temperature for recrystallization to obtain an orange solid **3a** (0.26 g, 20%). Mp = 92−95 °C. ^1H NMR ($CDCl_3$, 400 MHz): δ 0.86 (t, J = 6.8 Hz, 6 H), 1.25−1.37 (m, 24 H), 1.51−1.55 (m, 4 H), 1.70−1.73 (m, 4 H), 2.55 (t, J = 7.0 Hz, 4 H), 7.05 (d, J = 5.2 Hz, 2 H), 7.17 (d, J = 5.2 Hz, 2 H), 7.77 (s, 2 H), 8.13 (s, 2 H); ^{13}C NMR ($CDCl_3$, 100 MHz, ppm): δ 14.1, 20.0, 22.7, 28.5, 29.1, 29.3, 29.4, 29.6, 29.7, 31.9, 76.2, 96.6, 116.1, 119.8, 120.3, 123.9, 132.0, 136.7, 137.2, 137.7, 138.2; HRMS (EI, quadrupole, $C_{42}H_{50}S_4$): calcd, 682.2795; found, 682.2787.

DOI: 10.1021/acs.joc.6b00101
J. Org. Chem. 2016, 81, 2534−2542

*Synthesis of **3b**.* To a 100 mL two-neck bottom flask, compound **1** (1 g, 1.9 mmol), 3-bromo-2-(dodec-1-yn-1-yl)thiophene **2b** (1.52 g, 4.65 mmol), $Pd(PPh_3)_4$ (0.11 g, 0.096 mmol), and degassed toluene (40 mL) were introduced. The mixture was reacted at 130 °C under nitrogen for 12 h. After removal of solvent by a rotary evaporator, the residue was purified by column chromatography on silica gel (hexane/ethyl acetate, v/v, 50/1). The compound was dissolved in hexane at 60 °C. The solution was cooled down to room temperature for recrystallization to obtain an orange solid **3b** (0.68 g, 52%). Mp = 153−156 °C. ^{1}H NMR ($CDCl_3$, 400 MHz): δ 0.86 (t, J = 6.8 Hz, 6 H), 1.25−1.37 (m, 24 H), 1.50−1.55 (m, 4 H), 1.68−1.74 (m, 4 H), 2.59 (t, J = 7 Hz, 4 H), 7.19 (d, J = 5.6 Hz, 2 H), 7.30 (d, J = 5.6 Hz, 2 H), 7.85 (s, 2 H), 8.17 (s, 2 H); ^{13}C NMR ($CDCl_3$, 100 MHz, ppm): δ 14.1, 20.2, 22.7, 28.4, 29.1, 29.3, 29.4, 29.61, 29.64, 31.9, 74.2, 100.8, 116.2, 119.6, 120.4, 125.5, 126.8, 136.6, 136.9, 138.0, 138.3; HRMS (EI, quadrupole, $C_{42}H_{50}S_4$): calcd, 682.2795; found, 682.2792.

Synthesis of 6,13-syn-TBDT. **3a** (186 mg, 0.27 mmol) and degassed *N*-methyl-2-pyrrolidone (NMP, 18 mL) were placed in a 50 mL two-neck bottom flask. The mixture was heated to 180 °C, and 1,8-diazabicycloundec-7-ene (DBU, 0.05 mL, 0.29 mmol) was added to the flask. After reacting for 12 h at 180 °C, the mixture was poured into the saturated NH_4Cl aqueous solution (100 mL). The precipitate was collected and dissolved in hexane at 60 °C. The solution was cooled down to room temperature for recrystallization to obtain a dark-yellow solid 6,13-*syn*-TBDT (100 mg, 53%). Mp = 127 °C. ^{1}H NMR ($CDCl_3$, 400 MHz): δ 0.88 (t, J = 6.2 Hz, 6 H), 1.29−1.43 (m, 24 H), 1.56−1.61 (m, 4 H), 1.83−1.87 (m, 4 H), 3.28 (t, J = 7.6 Hz, 4 H), 7.38 (d, J = 5.2 Hz, 2 H), 7.47 (d, J = 5.2 Hz, 2 H), 7.60 (s, 2 H), 8.64 (s, 2 H); ^{13}C NMR ($CDCl_3$, 100 MHz, ppm): δ 14.1, 22.7, 29.4, 29.60, 29.65, 29.67, 29.71, 29.74, 32.0, 35.2, 118.2, 121.3, 124.4, 126.1, 129.5, 131.4, 134.4, 134.5, 136.3, 136.4, 138.6; HRMS (EI, quadrupole, $C_{42}H_{50}S_4$): calcd, 682.2795; found, 682.2794.

Synthesis of 6,13-anti-TBDT. **3b** (0.6 g, 0.88 mmol) and degassed *N*-methyl-2-pyrrolidone (NMP, 60 mL) were placed in a two-neck bottom flask. The mixture was heated to 180 °C, and 1,8-diazabicycloundec-7-ene (DBU, 0.15 mL, 0.97 mmol) was added to the flask. After reacting for 12 h at 180 °C, the mixture was poured into the saturated NH_4Cl aqueous solution (250 mL). The precipitate was collected and dissolved in hexane at 60 °C. The solution was cooled down to room temperature for recrystallization to obtain a pale-yellow solid 6,13-*anti*-TBDT (0.38 g, 63%). Mp = 191 °C. ^{1}H NMR ($CDCl_3$, 600 MHz): δ 0.88 (t, J = 6.6 Hz, 6 H), 1.26−1.38 (m, 20 H), 1.44−1.50 (m,4 H), 1.62−1.65 (m, 4 H), 1.93−1.96 (m, 4 H), 3.43 (t, J = 7.5 Hz, 4 H), 7.55 (d, J = 5.4 Hz, 2 H), 7.56 (d, J = 5.4 Hz, 2 H), 7.76 (s, 2 H), 8.83 (s, 2 H); ^{13}C NMR ($CDCl_3$, 150 MHz, ppm): δ 14.1, 22.7, 29.3, 29.60, 29.65, 29.67, 29.75, 29.80, 32.0, 35.5, 118.3, 119.9, 121.8, 126.6, 129.4, 132.4, 134.7, 135.7, 136.4, 136.6, 138.5; HRMS (EI, quadrupole, $C_{42}H_{50}S_4$): calcd, 682.2795; found, 682.2805.

*Synthesis of **6a**.* To a two-neck bottom flask, compound **4** (0.3 g, 1.37 mmol), $PdCl_2(PPh_3)_2$ (48 mg, 0.068 mmol), CuI (26 mg, 0.137 mmol), 2-iodothiophene (**5a**, 606 mg, 2.88 mmol), degassed THF (15 mL), and diisopropylamine (15 mL) were introduced. The mixture was stirred at room temperature under nitrogen for 30 min. After quenching the reaction by water, the mixture was extracted by brine and saturated NH_4Cl aqueous solution. The combined organic layers were dried with $MgSO_4$, and the solvent was removed under reduced pressure. The crude product was washed by methanol and hexane to obtain a dark-yellow solid **6a** (460 mg, 88%). Mp = 176−178 °C. ^{1}H NMR ($CDCl_3$, 400 MHz): δ 2.53 (s, 6 H), 7.04 (dd, J_1 = 5.2 Hz, J_2 = 3.6 Hz, 2 H), 7.26 (d, J = 3.6 Hz, 2 H), 7.34 (s, 2 H), 7.34 (d, J = 5.2 Hz, 2 H); ^{13}C NMR ($CDCl_3$, 100 MHz, ppm): δ 15.5, 90.3, 90.7, 121.9, 122.7, 127.2, 127.9, 128.1, 132.4, 137.6.; HRMS (EI, quadrupole, $C_{20}H_{14}S_4$): calcd, 381.9978; found, 381.9975.

*Synthesis of **7a**.* **6a** (0.3 g, 0.78 mmol) and iodine (0.5 g, 1.96 mmol) were placed in a 100 mL round-bottom flask with dichloromethane (30 mL). After reacting at ambient temperature for 3 h, the mixture was extracted with brine and dichloromethane. The combined organic layers were dried over $MgSO_4$, and the solvent was removed under reduced pressure. The crude product was washed by methanol, hexane, and ether to obtain a dark-brown solid **7a** (0.38 g, 80%). Mp = 244−246 °C. ^{1}H NMR ($CDCl_3$, 400 MHz): δ 7.17 (dd, J_1 = 5.0 Hz, J_2 = 3.8 Hz, 2H), 7.48 (dd, J_1 = 5.0 Hz, J_2 = 1.0 Hz, 2 H), 7.64 (dd, J_1 = 3.6 Hz, J_2 = 0.8 Hz, 2 H), 8.16 (s, 2 H); HRMS (EI, quadrupole, $C_{18}H_8I_2S_4$): calcd, 605.7598; found, 605.7603; ^{13}C NMR is not available due to the poor solubility.

*Synthesis of **8a**.* To a 50 mL two-neck bottom flask, **7a** (1 g, 1.65 mmol), $Pd(PPh_3)_4$ (190 mg, 0.17 mmol), CuI (32 mg, 0.17 mmol), degassed toluene (15 mL), and diisopropylamine (DIPA, 15 mL) were introduced. 1-Dodecyne (658 mg, 3.96 mmol) was added to the mixture, and the contents were stirred at 80 °C under nitrogen for 16 h. The solvent was removed under reduced pressure, and the crude product was purified by column chromatography on silica gel (hexane/ethyl acetate, v/v, 50/1). The compound was dissolved in hexane at 60 °C. The solution was cooled down to room temperature for recrystallization to obtain an orange **8a** (0.21 g, 19%). Mp = 83−85 °C. ^{1}H NMR ($CDCl_3$, 400 MHz): δ 0.88 (t, J = 6.8 Hz, 6 H), 1.29−1.40 (m, 24 H), 1.55−1.59 (m, 4 H), 1.76−1.79 (m, 4 H), 2.66 (t, J = 6.8 Hz, 4 H), 7.11 (dd, J_1 = 4.8 Hz, J_2 = 4 Hz, 2 H), 7.39 (d, J = 4.8 Hz, 2 H), 7.62 (d, J = 4 Hz, 2 H), 8.16 (s, 2 H); ^{13}C NMR ($CDCl_3$, 100 MHz, ppm): δ 14.1, 20.1, 22.7, 28.6, 29.2, 29.3, 29.4, 29.6, 31.9, 74.9, 100.0, 112.6, 115.9, 126.5, 126.7, 127.1, 134.6, 136.6, 139.2, 139.5; HRMS (EI, quadrupole, $C_{42}H_{50}S_4$): calcd, 682.2795; found, 682.2800.

Synthesis of 7, 14-syn-TBDT. **8a** (150 mg, 0.21 mmol) and degassed *N*-methyl-2-pyrrolidone (NMP, 15 mL) were placed in the 50 mL two-neck bottom flask. The mixture was heated to 180 °C, and 1,8-diazabicycloundec-7-ene (DBU, 35 mg, 0.23 mmol) was added to the flask. After reacting 12 h at 180 °C, the mixture was poured into the saturated NH_4Cl aqueous solution (100 mL). The precipitate was collected and dissolved in hexane at 60 °C. The solution was cooled down to room temperature for recrystallization to obtain a dark-yellow solid 7,14-*syn*-TBDT (98 mg, 65%). Mp = 178 °C. ^{1}H NMR ($CDCl_3$, 400 MHz): δ 0.88 (t, J = 6.8 Hz, 6 H), 1.28−1.39 (m, 24 H), 1.44−1.48 (m, 4 H), 1.81−1.85 (m, 4 H), 3.10 (t, J = 8 Hz, 4 H), 7.52 (d, J = 5.6 Hz, 2 H), 7.57 (d, J = 5.6 Hz, 2 H), 7.96 (s, 2 H), 8.63 (s, 2 H); ^{13}C NMR ($CDCl_3$, 100 MHz, ppm): δ 14.1, 22.7, 29.3, 29.57, 29.63, 29.7, 31.2, 31.9, 34.4, 115.6, 117.5, 123.1, 125.3, 131.2, 131.8, 133.6, 135.2, 135.4, 136.1, 138.7; HRMS (EI, quadrupole, $C_{42}H_{50}S_4$): calcd, 682.2795; found, 682.2753.

*Synthesis of **6b**.* To a 50 mL two-neck bottom flask, **4** (0.5 g, 2.29 mmol), $PdCl_2(PPh_3)_2$ (80 mg, 0.12 mmol), CuI (44 mg, 0.22 mmol), degassed THF (8 mL), and diisopropylamine (DIPA, 8 mL) were introduced. 3-Iodothiophene (**5b**, 1.01 g, 4.8 mmol) was added to the mixture, and the contents were stirred at room temperature under nitrogen for 30 min. After quenching the reaction by water, the mixture was extracted by brine and saturated NH_4Cl aqueous solution. The combined organic layers were dried over $MgSO_4$, and the solvent was removed under reduced pressure. The crude product was washed by methanol and hexane to obtain a dark-yellow solid **6b** (0.72 g, 82%). Mp = 193−197 °C. ^{1}H NMR ($CDCl_3$, 400 MHz): δ 2.52 (s, 6 H), 7.23 (d, J = 4.8 Hz, 2 H), 7.25 (s, 2 H),, 7.33 (dd, J_1 = 4.8, J_2 = 1.6 Hz, 2 H) 7.58 (d, J = 1.6 Hz, 2 H); ^{13}C NMR ($CDCl_3$, 100 MHz, ppm): δ 15.4, 86.2, 92.6, 121.8, 122.0, 125.5, 127.9, 129.2, 129.8, 137.5; HRMS (EI, quadrupole, $C_{20}H_{14}S_4$): calcd, 381.9978; found, 381.9983.

*Synthesis of **7b**.* **6b** (1 g, 2.61 mmol) and iodine (1.65 g, 6.53 mmol) were placed in a 250 mL round-bottom flask with dichloromethane (100 mL). After reacting at ambient temperature for 3 h, the mixture was extracted with brine and dichloromethane. The combined organic layers were dried over $MgSO_4$, and the solvent was removed under reduced pressure. The crude product was washed by methanol, hexane, and ether to give a dark-brown solid **7b** (1.2 g, 76%). Mp = 223−226 °C. ^{1}H NMR ($CDCl_3$, 400 MHz): δ 7.45 (dd, J_1 = 2.8, J_2 = 4.8 Hz, 2 H), 7.60 (dd, J_1 = 1.2, J_2 = 4.8 Hz, 2 H), 7.90 (dd, J_1 = 1.2 Hz, J_2 = 2.8 Hz, 2 H), 8.20 (s, 2 H); ^{13}C NMR is not available due to the poor solubility; HRMS (EI, quadrupole, $C_{18}H_8I_2S_4$): calcd, 605.7598; found, 605.7599.

*Synthesis of **8b**.* To a 100 mL two-neck bottom flask, **7b** (1 g, 1.65 mmol), Pd $(PPh_3)_4$ (190 mg, 0.17 mmol), CuI (32 mg, 0.17 mmol),

DOI: 10.1021/acs.joc.6b00101
J. Org. Chem. 2016, 81, 2534−2542

degassed toluene (15 mL), and diisopropylamine (DIPA, 15 mL) were introduced. The mixture was added 1-dodecyne (658 mg, 3.96 mmol) and stirred at 80 °C under nitrogen for 12 h. The solvent was removed under reduced pressure, and the crude product was purified by column chromatography on silica gel (hexane/ethyl acetate, v/v, 50/1). The compound was dissolved in hexane at 60 °C. The solution was cooled down to room temperature for recrystallization to obtain an orange solid **8b** (0.42 g, 37%). Mp = 79−82 °C. ^{1}H NMR ($CDCl_3$, 400 MHz): δ 0.86 (m, 6 H), 1.26−1.38 (m, 24 H), 1.53−1.56 (m, 4 H), 1.73−1.77 (m, 4 H), 2.63 (t, J = 7.2 Hz, 4 H), 7.40 (dd, J_1 = 5.0 Hz, J_2 = 3.0 Hz, 2 H), 7.78 (dd, J = 5.2 Hz, J_2 = 1.2 Hz, 2 H), 8.07 (dd, J_1 = 2.6, J_2 = 1.0 Hz, 2 H), 8.23 (s, 2 H); ^{13}C NMR ($CDCl_3$, 100 MHz, ppm): δ 14.1, 19.9, 22.7, 28.8, 29.1, 29.2, 29.4, 29.6, 31.9, 75.3, 97.4, 112.7, 116.0, 123.5, 125.7, 127.1, 134.7, 135.0, 139.7, 140.7; HRMS (EI, quadrupole, $C_{42}H_{50}S_4$): calcd, 682.2795; found, 682.2799.

Synthesis of 7, 14-anti-TBDT. **8b** (100 mg, 0.14 mmol) and degassed *N*-methyl-2-pyrrolidone (NMP, 10 mL) were placed in a 50 mL two-neck bottom flask. The mixture was heated to 180 °C, and 1,8-diazabicycloundec-7-ene (DBU, 25 mg, 0.16 mmol) was added. After reacting for 12 h at 180 °C, the mixture was poured into saturated NH_4Cl aqueous solution (100 mL). The precipitate was collected and dissolved in THF at 60 °C. The solution was cooled down to room temperature for recrystallization to give a dark-yellow solid **7**, 14-*anti*-TBDT (35 mg, 35%). Mp = 234 °C. ^{1}H NMR ($CDCl_3$, 600 MHz): δ 0.83−0.89 (m, 6 H), 1.28−1.30 (m, 20 H), 1.40−1.42 (m, 4 H), 1.47−1.51 (m, 4 H), 1.92−1.94 (m, 4 H), 3.07 (t, J = 7.8 Hz, 4 H), 7.62 (m, 4 H), 7.99 (s, 2 H), 8.69 (s, 2 H); ^{13}C NMR ($CDCl_3$, 150 MHz, ppm): δ 14.0, 22.6, 29.3, 29.46, 29.49, 29.53, 29.6, 31.9, 35.2, 115.4, 116.7, 122.5, 127.0, 132.0, 132.3, 133.7, 134.0, 135.3, 136.2, 139.3; HRMS (EI, quadrupole, $C_{42}H_{50}S_4$): calcd, 682.2795; found, 682.2793.

Synthesis of TD-syn-TBDT. To a 50 mL round-bottom flask, **7a** (150 mg, 0.17 mmol), 11-docosyne (454 mg, 1.48 mmol), pivalic acid (25 mg, 0.25 mmol), K_2CO_3 (204 mg, 1.48 mmol), $Pd(OAc)_2$ (2.7 mg, 0.01 mmol), and degassed dimethylacetamide (DMAc,10 mL) were introduced. The mixture was heated to 120 °C under nitrogen for 16 h. After quenching the reaction by water, the mixture was extracted by brine and saturated NH_4Cl aqueous solution. The combined organic layers were dried over $MgSO_4$ and the solvent was removed under reduced pressure. The crude product was purified by column chromatography on silica gel (hexane as eluent). The compound was dissolved in hexane at 60 °C. The solution was cooled down to room temperature for recrystallization to obtain a yellow solid TD-*syn*-TBDT (85 mg, 36%). Mp = 102 °C. ^{1}H NMR ($CDCl_3$, 400 MHz): δ 0.86−0.91 (m, 12 H), 1.23−1.41 (m, 44 H), 1.47−1.57 (m, 8 H), 1.69−1.74 (m, 8 H), 1.80 (m, 4 H), 3.09 (t, J = 8 Hz, 4 H), 3.35 (t, J = 8 Hz, 4 H), 7.47(d, J = 5.2 Hz, 2 H), 7.49 (d, J = 5.2 Hz, 2 H), 8.70 (s, 2 H); ^{13}C NMR ($CDCl_3$, 100 MHz, ppm): δ 14.1, 14.2, 22.69, 22.73, 29.4, 29.5, 29.6, 29.7, 29.72, 30.0, 30.1, 30.2, 30.5, 31.7, 31.9, 32.0, 118.4, 123.7, 125.6, 130.2, 131.4, 132.3, 132.8, 133.8, 134.5, 136.4, 138.7; HRMS (FAB, quadrupole, $C_{62}H_{90}S_4$): calcd, 962.5925; found, 962.5927.

Synthesis of TD-anti-TBDT. To a 100 mL round-bottom flask, **7b** (500 mg, 0.83 mmol), 11-docosyne (1.01 g, 3.3 mmol), pivalic acid (168 mg, 1.65 mmol), K_2CO_3 (456 mg, 3.3 mmol), $Pd(OAc)_2$ (18.5 mg, 0.08 mmol), and degassed dimethylacetamide (DMAc, 25 mL) were introduced. The mixture was heated to 120 °C under nitrogen for 16 h. After quenching the reaction by water, the mixture was extracted by brine and saturated NH_4Cl aqueous solution. The combined organic layers were dried over $MgSO_4$, and the solvent was removed under reduced pressure. The crude product was purified by column chromatography on silica gel (hexane as eluent). The compound was dissolved in hexane at 60 °C. The solution was cooled down to room temperature for recrystallization to obtain a yellow solid TD-*anti*-TBDT (205 mg, 26%). Mp = 150 °C. ^{1}H NMR ($CDCl_3$, 400 MHz): δ 0.88−0.89 (m, 12 H), 1.30−1.43 (m, 44 H), 1.53−1.57 (m, 8 H), 1.71−1.87 (m, 12 H), 3.08 (t, J = 8.0 Hz, 4 H), 3.42 (t, J = 7.6 Hz, 4 H), 7.54 (d, J = 5.2 Hz, 2 H), 7.56 (d, J = 5.2 Hz, 2 H), 8.80 (s, 2 H). ^{13}C NMR ($CDCl_3$, 100 MHz, ppm): δ 14.1, 22.69, 22.71, 29.38, 29.46, 29.51, 29.64, 29.67, 29.71, 29.9, 30.08, 30.13, 30.2, 31.9, 32.0, 32.8, 118.3, 122.6, 126.1, 130.2, 131.5, 131.7, 133.5, 133.6, 134.4, 136.5, 140.1; HRMS (FAB, quadrupole, $C_{62}H_{90}S_4$): calcd, 962.5930; found, 962.5931.

Fabrication and Characterization of OFET Devices. 300 nm-thick SiO_2 was deposited on the n-doped silicon wafer (C_i = 1.1 nF cm^{-2}). The substrates were rinsed at room temperature for an hour in a 3:1 (volume ratio) sulfuric acid and hydrogen peroxide (30% solution in water), followed by 15 min of sonication in pure water. After cleaning, the substrates were heated on a hot plate at 150 °C to remove water in a glovebox. Prior to growing the self-assembled monolayer with ODTS, the substrates underwent UV-ozone treatment for 30 min. Organic semiconductors were dissolved in chloroform (20 mg mL^{-1}) and spin-coated at 2000 rpm on the substrates. The architecture of field-effect transistors is bottom-gate/top-contact. On the top of the organic thin film, gold films (40 nm) as drain and source electrodes were deposited through a shadow mask. The drain−source channel length (L) and width (W) are 100 and 1000 μm, respectively. Characterization of OFET devices were carried out at room temperature under ambient conditions. The field-effect mobility was calculated in the saturation regime by using the equation $I_{ds} = C_i\mu(W/2L)(V_g - V_t)^2$, where I_{ds} is drain-source current, μ is the field-effect current, W is the channel width, L is the channel length, C_i is the capacitance per unit area of the gate dielectric layer, V_g is the gate voltage, and V_t is the threshold voltage.

■ ASSOCIATED CONTENT

Supporting Information

The Supporting Information is available free of charge on the ACS Publications website at DOI: 10.1021/acs.joc.6b00101.

Computational details, TGA analysis, and ^{1}H and ^{13}C NMR spectra (PDF)
Crystallographic data (CIF)
Crystallographic data (CIF)
Crystallographic data (CIF)

■ AUTHOR INFORMATION

Corresponding Author

*E-mail: yjcheng@mail.nctu.edu.tw.

Notes

The authors declare no competing financial interest.

■ ACKNOWLEDGMENTS

We thank the Ministry of Science and Technology and the Ministry of Education and Center for Interdisciplinary Science (CIS) of the National Chiao Tung University, Taiwan, for financial support. We thank the National Center of High-performance Computing (NCHC) in Taiwan for computer time and facilities. We thank Prof. Sue-Lein Wang at National Tsing Hua Uuiversity (NTHU) for help with the X-ray crystallography. Y.-J.C. thanks the support from the Golden-Jade fellowship of the Kenda Foundation, Taiwan.

■ DEDICATION

This article is dedicated to Professor Tien-Yau Luh on the occasion of his 70th birthday.

■ REFERENCES

(1) (a) Rieger, R.; Beckmann, D.; Mavrinskiy, A.; Kastler, M.; Müllen, K. *Chem. Mater.* **2010**, *22*, 5314−5318. (b) Zhou, H.; Yang, L.; Stuart, A. C.; Price, S. C.; Liu, S.; You, W. *Angew. Chem., Int. Ed.* **2011**, *50*, 2995−2998. (c) Zhang, S.; Ye, L.; Zhao, W.; Liu, D.; Yao, H.; Hou, J. *Macromolecules* **2014**, *47*, 4653−4659. (d) Huo, L. J.; Hou, J. H.; Zhang, S. Q.; Chen, H. Y.; Yang, Y. *Angew. Chem., Int. Ed.* **2010**, *49*, 1500−1503. (e) Liang, Y. Y.; Xu, Z.; Xia, J. B.; Tsai, S. T.; Wu, Y.; Li, G.; Ray, C.; Yu, L. P. *Adv. Mater.* **2010**, *22*, E135−E138. (f) Piliego,

DOI: 10.1021/acs.joc.6b00101
J. Org. Chem. 2016, 81, 2534−2542

C.; Holcombe, T. W.; Douglas, J. D.; Woo, C. H.; Beaujuge, P. M.; Fréchet, J. M. J. *J. Am. Chem. Soc.* **2010**, *132*, 7595−7597.
(2) (a) Roncali, J. *Chem. Rev.* **1997**, *97*, 173−206. (b) Forster, M.; Annan, K. O.; Scherf, U. *Macromolecules* **1999**, *32*, 3159. (c) Wu, J.-S.; Cheng, S.-W.; Cheng, Y.-J.; Hsu, C.-S. *Chem. Soc. Rev.* **2015**, *44*, 1113−1154. (d) Lee, C.-H.; Lai, Y.-Y.; Cheng, S.-W.; Cheng, Y.-J. *Org. Lett.* **2014**, *16*, 936−939. (e) Cheng, Y.-J.; Chen, C.-H.; Ho, Y.-J.; Chang, S.-W.; Vitek, A. H.; Hsu, C.-S. *Org. Lett.* **2011**, *13*, 5484−5487. (f) Cheng, Y.-J.; Chen, C.-H.; Lin, Y.-S.; Chang, C.-Y.; Hsu, C.-S. *Chem. Mater.* **2011**, *23*, 5068−5075. (g) Zhou, Y.; Liu, W.-J.; Ma, Y.; Wang, H.; Qi, L.; Cao, Y.; Wang, J.; Pei, J. *J. Am. Chem. Soc.* **2007**, *129*, 12386−12387. (h) Zhang, W.; Smith, J.; Watkins, S. E.; Gysel, R.; McGehee, M.; Salleo, A.; Kirkpatrick, J.; Ashraf, S.; Anthopoulos, T.; Heeney, M.; McCulloch, I. *J. Am. Chem. Soc.* **2010**, *132*, 11437−11439. (i) Li, Y.; Yao, K.; Yip, H.-L.; Ding, F.-Z.; Xu, Y.-X.; Li, X.; Chen, Y.; Jen, A. K.-Y. *Adv. Funct. Mater.* **2014**, *24*, 3631−3638. (j) Freund, T.; Scherf, U.; Mullen, K. *Angew. Chem., Int. Ed. Engl.* **1994**, *33*, 2424−2426. (k) Freund, T.; Mullen, K.; Scherf, U. *Macromolecules* **1995**, *28*, 547−551.
(3) (a) Chen, Y. L.; Chang, C. Y.; Cheng, Y. J.; Hsu, C. S. *Chem. Mater.* **2012**, *24*, 3964−3971. (b) Chen, Y.-L.; Kao, W.-S.; Tsai, C.-E.; Lai, Y.-Y.; Cheng, Y.-J.; Hsu, C.-S. *Chem. Commun.* **2013**, *49*, 7702−7704.
(4) Najari, A.; Beaupre, S.; Berrouard, P.; Zou, Y.; Pouliot, J. R.; Perusse, C. L.; Leclerc, M. *Adv. Funct. Mater.* **2011**, *21*, 718−728.
(5) (a) Chang, C.-Y.; Cheng, Y.-J.; Hung, S.-H.; Wu, J.-S.; Kao, W.-S.; Lee, C.-H.; Hsu, C.-S. *Adv. Mater.* **2012**, *24*, 549−553. (b) Cheng, Y.-J.; Wu, J.-S.; Shih, P.-I.; Chang, C.-Y.; Jwo, P.-C.; Kuo, W.-S; Hsu, C.-S. *Chem. Mater.* **2011**, *23*, 2361−2369. (c) Wang, Y.; Burton, D. J. *Org. Lett.* **2006**, *8*, 5295−5298. (d) Xu, J.; Wang, Y.; Burton, D. J. *Org. Lett.* **2006**, *8*, 2555−2558.
(6) (a) Osaka, I.; Houchin, Y.; Yamashita, M.; Kakara, T.; Takemura, N.; Koganezawa, T.; Takimiya, K. *Macromolecules* **2014**, *47*, 3502−3510. (b) Osaka, I.; Abe, T.; Shinamura, S.; Takimiya, K. *J. Am. Chem. Soc.* **2011**, *133*, 6852−6860. (c) Cheng, S.-W.; Chiu, D.-Y.; Tsai, C.-E.; Liang, W.-W.; Hsu, C.-Y.; Lai, Y.-Y.; Hsu, C.-S.; Osaka, I.; Takimiya, K.; Cheng, Y.-J. *Adv. Funct. Mater.* **2015**, *25*, 6131−6143. (d) Mamada, M.; Minamiki, T.; Katagiri, H.; Tokito, S. *Org. Lett.* **2012**, *14*, 4062−4065. (e) Lehnherr, D.; Waterloo, A. R.; Goetz, K. P.; Payne, M. M.; Hampel, F.; Anthony, J. E.; Jurchescu, O. D.; Tykwinski, R. R. *Org. Lett.* **2012**, *14*, 3660−3663.
(7) (a) Chang, H.-H.; Tsai, C.-E.; Lai, Y.-Y.; Liang, W.-W.; Hsu, S.-L.; Hsu, C.-S.; Cheng, Y.-J. *Macromolecules* **2013**, *46*, 7715−7726. (b) Graham, K. R.; Cabanetos, C.; Jahnke, J. P.; Idso, M. N.; Labban, A. E.; Ndjawa, G. O. N.; Heumueller, T.; Vandewal, K.; Salleo, A.; Chmelka, B. F.; Amassian, A.; Beaujuge, P. M.; McGehee, M. D. *J. Am. Chem. Soc.* **2014**, *136*, 9608−9618. (c) Li, J.; Qiao, X.; Xiong, Y.; Li, H.; Zhu, D. *Chem. Mater.* **2014**, *26*, 5782−5788. (d) Mei, J.; Bao, Z. *Chem. Mater.* **2014**, *26*, 604−615. (e) Kline, R. J.; DeLongchamp, D. M.; Fischer, D. A.; Lin, E. K.; Richter, L. J.; Chabiny, M. L.; Toney, M. F.; Heeney, M.; McCulloch, I. *Macromolecules* **2007**, *40*, 7960−7965.
(8) (a) Lai, Y.-Y.; Chang, H.-H.; Lai, Y.-Y.; Liang, W.-W.; Tsai, C.-E.; Cheng, Y.-J. *Macromolecules* **2015**, *48*, 6994−7006. (b) Wang, Y.; Burton, D. J. *Org. Lett.* **2006**, *8*, 5295−5298. (c) Xu, J.; Wang, Y.; Burton, D. J. *Org. Lett.* **2006**, *8*, 2555−2558.
(9) (a) Wu, J.-S.; Lin, C.-T.; Wang, C.-L.; Cheng, Y.-J.; Hsu, C.-S. *Chem. Mater.* **2012**, *24*, 2391−2399. (b) Wu, J.-S.; Lai, Y.-Y.; Cheng, Y.-J.; Chang, C.-Y.; Wang, C.-L.; Hsu, C.-S. *Adv. Energy Mater.* **2013**, *3*, 457−465. (c) Shimizu, M.; Nagao, I.; Tomioka, Y.; Hiyama, T. *Angew. Chem., Int. Ed.* **2008**, *47*, 8096.
(10) Larock, R. C.; Doty, M. J.; Tian, Q.; Zenner, J. M. *J. Org. Chem.* **1997**, *62*, 7536.
(11) Lafrance, M.; Fagnou, K. *J. Am. Chem. Soc.* **2006**, *128*, 16496−16497.

DOI: 10.1021/acs.joc.6b00101
J. Org. Chem. 2016, 81, 2534−2542